Synchronization between arterial blood pressure and cerebral oxyhaemoglobin concentration investigated by wavelet cross-correlation

A B Rowley[1,2]**, S J Payne**[1]**, I Tachtsidis**[3]**, M J Ebden**[1]**, J P Whiteley**[2]**, D J Gavaghan**[2]**, L Tarassenko**[1]**, M Smith**[4]**, C E Elwell**[3] **and D T Delpy**[3]

[1] Department of Engineering Science, University of Oxford, Parks Road, Oxford, OX1 3PJ, UK
[2] Computing Laboratory, University of Oxford, Parks Road, Oxford, OX1 3QD, UK
[3] UCL Department of Medical Physics and Bioengineering, Malet Place Engineering Building, Gower Street, London, WC1E 6BT, UK
[4] Department of Neuroanaesthesia and Neurocritical Care, The National Hospital for Neurology and Neurosurgery, Queen Square, London, WC1N 3BG, UK

E-mail: abr@robots.ox.ac.uk

Abstract
Wavelet cross-correlation (WCC) is used to analyse the relationship between low-frequency oscillations in near-infrared spectroscopy (NIRS) measured cerebral oxyhaemoglobin (O_2Hb) and mean arterial blood pressure (MAP) in patients suffering from autonomic failure and age-matched controls. Statistically significant differences are found in the wavelet scale of maximum cross-correlation upon posture change in patients, but not in controls. We propose that WCC analysis of the relationship between O_2Hb and MAP provides a useful method of investigating the dynamics of cerebral autoregulation using the spontaneous low-frequency oscillations that are typically observed in both variables without having to make the assumption of stationarity of the time series. It is suggested that for a short-duration clinical test previous transfer-function-based approaches to analyse this relationship may suffer due to the inherent nonstationarity of low-frequency oscillations that are observed in the resting brain.

Keywords: near-infrared spectroscopy, time frequency analysis, wavelet cross-correlation, posture changes, spontaneous oscillations, sympathetic stimulation, cerebral circulation

(Some figures in this article are in colour only in the electronic version)

1. Introduction

Cerebral autoregulation describes the regulatory response of cerebral haemodynamic variables to changes in blood pressure and is thought to be impaired in patients suffering from failure of the sympathetic nervous system (Panerai 1998). An analysis technique is desired which can quantify the status of cerebral autoregulation from the often noisy and short-duration measures of cardiovascular and haemodynamic variables obtained in the course of a head-up tilt table test, a routine clinical procedure for the assessment of patients suffering from sympathetic impairment (Jaradeh and Prieto 2003). Previous attempts have been made to quantify cerebral autoregulation in these patients by looking at absolute changes in cerebral blood flow and mean arterial pressure (for a comprehensive review see Panerai (1998)); however, the noise that is inherent in the data means that repetitions of the test would be required for a single patient study. This is neither practical nor ethical in the case of patients suffering from failure of the autonomic nervous system (Panerai 1998). This has led to a body of literature attempting to assess the status of autoregulation by considering the dynamic relationship between the spontaneous oscillations in cerebral blood flow that are know to occur in the resting brain and their counterparts in mean arterial blood pressure and heart rate.

There are a wide range of mechanisms which are thought to lead to low-frequency spontaneous oscillations in cerebral haemodynamics. The sources of these oscillations are poorly understood, and explanations for the source of an oscillation at a given frequency are multiple, and often controversial. Giller *et al* (1999) reported very low-frequency oscillations in cerebral blood flow (CBF) detected using transcranial ultrasonography (TCD) in humans and identify frequency bands centred around 0.0064 Hz, 0.02 Hz and 0.037 Hz that are synchronous throughout the cerebral vascular bed, yet not related to oscillations in blood pressure or CO_2. Hudetz *et al* (1992) report oscillations in CBF measured using laser Doppler flowmetry (LDF) within a frequency range of 0.06–0.1833 Hz in anaesthetized rats when blood pressure is held constant below 90 mmHg. Mayhew *et al* (1996) use reflected light imaging to investigate 0.1 Hz oscillations in the exposed cerebral cortex of rat and cat. Obrig *et al* (2000) demonstrate that similar oscillations may be captured non-invasively in the human brain using near-infrared spectroscopy (NIRS) to measure cerebral oxyhaemoglobin concentration (O_2Hb) and (Elwell *et al* 1999) underlined the implications of these oscillations for functional activation studies. It is suggested that oscillations in this region can be attributed to spontaneous vasomotion of cerebral vessels which may become entrained throughout the vasculature (Haddock and Hill 2005, Nilsson and Aalkjaer 2003) and should not be confused with similar low-frequency pressure waves (Nilsson and Aalkjaer 2003).

Within the same frequency region, however, high variability in blood pressure and heart rate is also found. Low-frequency cardiovascular variability in humans is typically observed within two frequency regions (Cohen and Taylor 2002). The first is thought to be respiratory related and occurs at a frequency of around 0.3 Hz. The second is thought to be due to the action of the sympathetic nervous system and is centred at around 0.1 Hz (Stauss *et al* 1998, Malliani *et al* 1991, Pagani *et al* 1986, Nilsson and Aalkjaer 2003, Cohen and Taylor 2002). Mayer (1876) was the first to report slow waves in blood pressure at around this frequency hence cardiovascular oscillations in this frequency region are often termed Mayer or M-waves. Impairment of the action of the sympathetic nervous system has been shown in a number of studies to reduce the M-wave component of cardiovascular variability (Elghozi *et al* 1991, Chandler and Mathias 2002, Cencetti *et al* 1999, Kamiya *et al* 2005, Kawaguchi *et al* 2001). Since impairment of the sympathetic nervous system is observed in elderly patients, and associated with unexplained falls and syncope, bivariate relationships have been investigated between these oscillations in blood pressure and cerebral haemodynamics

typically using transfer function identification techniques (Panerai *et al* 1998, 2001, Simpson *et al* 2001, Mitsis and Marmarelis 2002, Mitsis *et al* 2002, 2004), and comparison of power spectral densities (Tachtsidis *et al* 2003, 2004). Tachtsidis *et al* (2003) report changes in low-frequency power of the spontaneous oscillations measured using NIRS with posture suggesting sympathetic influence on this variability.

The relationship between spontaneous low-frequency oscillations in the resting brain and cardiovascular variability currently appears to be the most promising technique of assessing the status of cerebral autoregulation non-invasively in patients, yet there are numerous sources which may give rise to this variability, not all of which can be attributed to variations in cardiovascular parameters. It has been suggested by a number of other researchers (Giller and Mueller 2003, Latka *et al* 2005, Hu *et al* 2006) that this could lead to a highly nonstationary relationship between cardiovascular and cerebral variability. Spontaneous oscillations have been assessed using a variety of modalities. The two prevalent non-invasive techniques for human studies are TCD and NIRS. TCD measures the velocity (VMCA) of blood flowing in the middle cerebral artery, whereas NIRS measures (among other things) an averaged tissue concentration (O_2Hb) in the illuminated region which consists of arterial, arteriolar, capillary and venous blood flow.

In this paper, the complex continuous Morlet wavelet transform is used to perform a multiresolution analysis of mean arterial blood pressure and NIRS-measured O_2Hb time series taken from sympathetic failure patients and age-matched controls undergoing passive posture changes induced by a head-up tilt table test. Cross-correlation is then used to derive a measure of linear relatedness between these variables as a function of wavelet scale (analogous to frequency) and time. This technique has been used for the assessment of coupling and synchronization between nonstationary geophysical oscillations (Grinsted *et al* 2004) and in the EEG (Mizuno-Matsumoto *et al* 2005) yet not for the assessment of autoregulation using NIRS. Since this technique does not make the assumption of stationarity for the relationship between the two time series it is suggested that it may provide a method which is more effective than the transfer function estimation techniques typically used for the assessment of cerebral autoregulation, particularly when used with time series obtained from short-duration head-up tilt table tests.

2. Clinical methods

The study utilized anonymized data from a previous investigation by our group in which changes in cerebral haemodynamics were measured with near-infrared spectroscopy during orthostatic hypotension (Tachtsidis *et al* 2005). The original study, approved by the Joint Research Ethics Committee of the National Hospital for Neurology and Neurosurgery and Institute of Neurology, included eight patients with autonomic failure (Schatz *et al* 1996) of mean age 42–79 years and eight healthy age-matched controls. Written consent was obtained from all participants prior to inclusion in the study. Passive head-up tilt using a tilt table is a routine diagnostic test in patients with autonomic failure (Jaradeh and Prieto 2003) and the study protocol in patients and controls consisted of 10 min of supine rest followed by 10 min of passive head-up tilt and a further 10 min of supine rest. The head-up tilt was reversed before 10 min if a patient developed syncope or pre-syncopal symptoms.

The continuous blood pressure waveform was monitored non-invasively for the duration of the test using finger photoplethysmography (Portapres$^®$, Ohmeda) at a sampling frequency of 100 Hz. A single-channel continuous wave near-infrared spectrometer with a sampling rate of 6 Hz (NIRO 300, Hamamatsu Photonics KK) was used to measure changes in O_2Hb using the modified Beer–Lambert law (Delpy and Cope 1997).
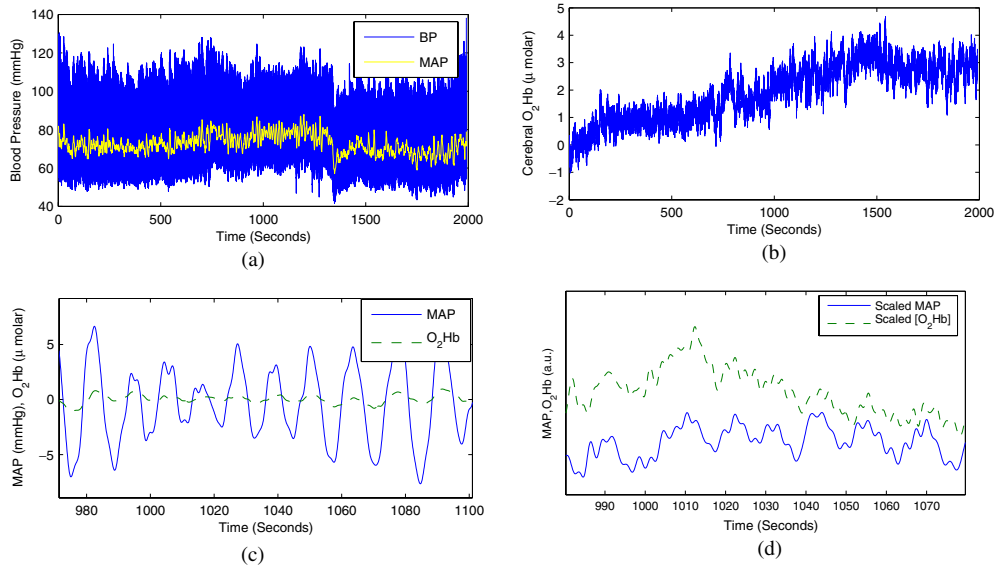
Figure 1. Time series measured from patients before and after pre-processing: (a) measured blood pressure (BP) and mean arterial pressure (MAP) time series, (b) measured O_2Hb time series, (c) comparison of MAP and O_2Hb time series indicating observed LF synchronization and (d) comparison of MAP and O_2Hb time series indicating observed VLF synchronization.

3. Data analysis

The measured blood pressure (BP) time series was converted to MAP using an automated peak and trough detection algorithm (Townsend and Germuska 2005), involving an adaptive rule-based search for the large gradient in blood pressure due to systole followed by waveform integration over the cardiac cycle. MAP and O_2Hb were resampled to 10 Hz using cubic spline interpolation. Sections of the time series having a duration of 400 s were selected manually for each posture to avoid transient effects caused by the subject or clinicians adjusting the subject's posture during the tilt phase. Each section of data was then high pass filtered using a fifth-order Butterworth filter with a cut-off frequency of 0.005 Hz to remove very slow variations and baseline shift (Mitsis *et al* 2004) and subsequently low pass filtered using a fifth-order Butterworth filter with a cut-off frequency of 0.8 Hz in order to remove variability in the signal due to the cardiac cycle. This pre-processing algorithm resulted in three pairs of pre-processed time series of 400 s duration at 10 Hz for each patient (MAP and O_2Hb before, during and after the tilt).

Typical time series before and after pre-processing are shown in figure 1. Figures 1(a) and (b) show typical records for the entire test duration. Figures 1(c) and (d) show short sections of the pre-processed time series that have been extracted to indicate the variability that is typically encountered. Figure 1(c) shows low-frequency (LF) oscillations having a period close to 10 s in both the MAP and O_2Hb time series. A similar LF variation can be seen in figure 1(d) but with an additional very-low-frequency (VLF) variation. It should be noted that in figure 1(d) the measured O_2Hb has been scaled by a factor of 10 and offset vertically to illustrate the synchronization between the VLF component of the oscillation in the two time series.

Power spectral densities were calculated for each of the pre-processed time series with the Welch technique (Welch 1967) with a 512-point (51.2 s) Hanning window with an overlap

of 256 points. Total power in the low-frequency (0.005–0.15 Hz) and high-frequency (0.15–0.5 Hz) regions of the spectrum was obtained by trapezoidal integration of the power spectral density.

Continuous complex Morlet wavelet transforms with centre frequency $f_c = 1$ were then computed for each time series at scales, a, with unit spacing from 20 to 250 (representing frequencies 0.5–0.04 Hz for time series sampled at 10 Hz) using the MATLAB$^®$ (Mathworks, Natick, MA) wavelet toolbox function cwt (Misiti *et al* 2004). This gave two complex time series, $W_{MAP}(a, t)$ and $W_{OHb}(a, t)$, for each segment of the test. Taking the complex argument of these time series gives a representation of the instantaneous phases, $\phi_{MAP}(a, t)$ and $\phi_{OHb}(a, t)$, as a function of wavelet scale and time (Le Van Quyen *et al* 2001). Taking the difference allows the instantaneous phase difference to be calculated as

$$\Delta\phi(a, t) = \phi_{MAP}(a, t) - \phi_{OHb}(a, t). \tag{1}$$

To analyse synchronization between the MAP and O$_2$Hb time series, the circular mean, $\overline{\Delta\phi(a)}$, of the phase difference over the duration of a test segment was calculated using

$$\overline{\Delta\phi(a)} = \tan^{-1}\left(\frac{\sum_t \sin(\Delta\phi(a, t))}{\sum_t \cos(\Delta\phi(a, t))}\right). \tag{2}$$

The synchronization index, $\gamma(a)$ (Latka *et al* 2005), which is an inverse circular statistical analogue of variance (see Fisher 1995) was calculated using

$$\gamma(a) = \frac{1}{N}\left(\left[\sum_t \cos(\Delta\phi(a, t))\right]^2 + \left[\sum_t \sin(\Delta\phi(a, t))\right]^2\right), \tag{3}$$

in which N is the number of time points in the series. The normalized wavelet cross-correlation $\overline{WCC}(a, \tau)$ was calculated using

$$\overline{WCC}(a, \tau) = \frac{|R_{X,Y}(W_{MAP}, W_{OHb}, a, \tau)|}{\sqrt{|R_{X,X}(W_{MAP}, a, 0) \cdot R_{X,X}(W_{OHb}, a, 0)|}}, \tag{4}$$

in which $R_{X,Y}(s1, s2, a, \tau)$ denotes the cross-correlation of the wavelet coefficients of time series $s1$ and $s2$ at a scale a for a relative time shift τ and $R_{X,X}(s1, a, \tau)$ denotes the auto-correlation of the time series $s1$ for a time shift τ.

$\overline{WCC}(a, \tau)$ represents the cross-spectral power in the two time series (shifted relative to each other by τ) as a fraction of the total power in the two time series. At a given wavelet scale $\overline{WCC}(a, \tau) = 1$ would indicate that the coefficients of the two wavelet transforms were related to each other by a simple scaling factor, suggesting strong synchronization at this frequency. For a more detailed explanation of wavelet cross-correlation see Grinsted *et al* (2004) and Maraun and Kurths (2004).

For each time series pair at each posture, the maximum value of $\overline{WCC}(a, \tau)$ was found, and the scale, a_{MAX}, and time delay, τ_{MAX}, at which this maximum occurred were recorded. For this scale of maximum wavelet cross-correlation, the values of the circular mean phase difference, $\overline{\Delta\phi(a_{MAX})}$, and the synchronization index, $\gamma(a_{MAX})$, were also calculated. A paired *t*-test (see Goulden (1959)) was then used to analyse the statistical significance of the differences in the group mean of each of these variables between controls and patients, and with posture changes.

4. Results

Figure 2 shows filled contour plots of the wavelet cross-correlation function $\overline{WCC}(a, \tau)$ for a typical control subject and an autonomic failure patient during supine rest and head-up tilt.
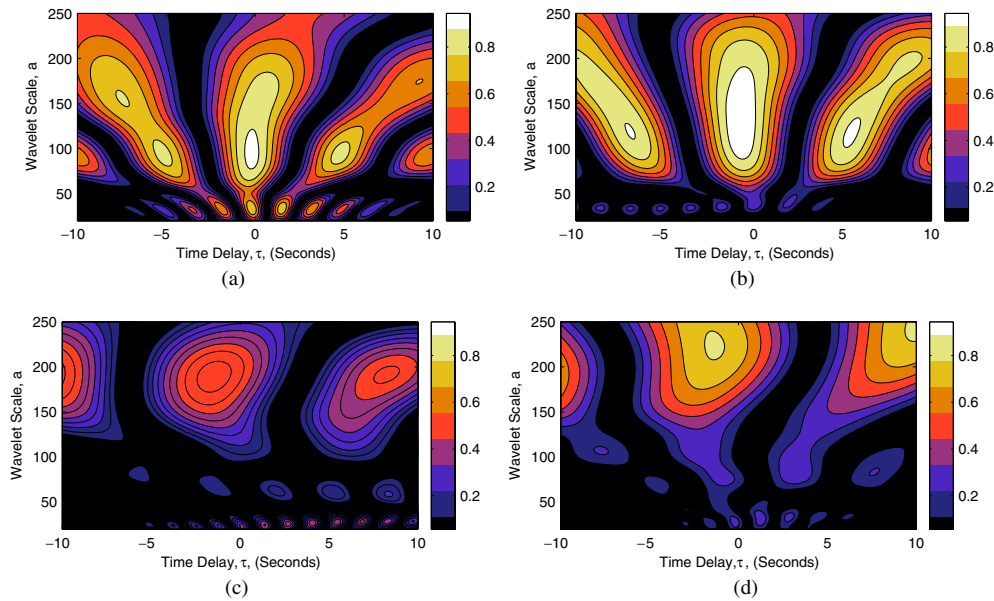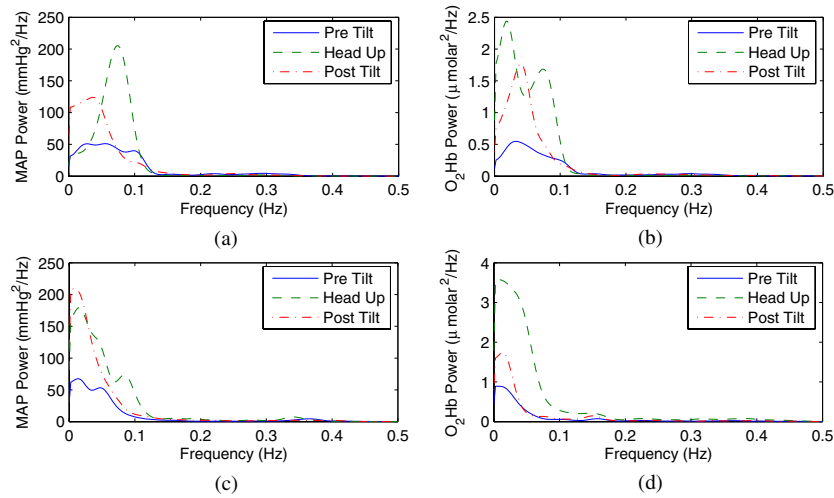
Figure 2. Wavelet cross-correlation between MAP and O$_2$Hb for a typical control subject and an autonomic failure patient: (a) healthy subject, supine, (b) healthy subject, head-up tilt, (c) autonomic failure patient, supine and (d) autonomic failure patient, head-up tilt.

For healthy subjects in the supine position before head-up tilt (figure 2(a)) peaks in the wavelet cross-correlation typically occur within two regions. The first peak typically occurs at a scale of around 30 (0.33 Hz) and possibly corresponds to the respiratory peak. The second peak typically occurs at a scale of around 100 (0.1 Hz) which could correspond to the Mayer wave peak. These results are in agreement with those of Latka *et al* (2005). Upon head-up tilt in healthy subjects (figure 2(b)) the level of cross-correlation at the respiratory peak reduces significantly, and the Mayer wave peak appears to spread to higher scales. There appears to be no discernible differences in the value of lag times at which these peaks occur.

In autonomic failure patients in the supine position (figure 2(c)) no respiratory peak is typically observed in the wavelet cross-correlation, and the most significant peak appears to be at a much higher scale of around 180 ($\simeq$0.05 Hz). The difference between the supine and head-up wavelet cross-correlation (figures 2(c) and (d)) appears more subtle for this patient. This point will be revisited in discussion of the group statistics.

Figure 3 shows power spectral density plots for the same subjects as displayed in figure 2. Figure 3(a) shows that power in the pre-tilt MAP time series for the healthy subject exists in the low-frequency region, for frequencies less than around 0.15 Hz, power in O$_2$Hb for this subject (figure 3(b)) shows a similar distribution however with a peak around 0.05 Hz that is slightly more pronounced than for MAP. For the head-up time series in the healthy subject spectral power in MAP (figure 3(a)) shows a strong peak close to 0.1 Hz, which is mirrored in the corresponding O$_2$Hb spectrum (figure 3(b)). The latter also shows an additional low-frequency peak that has shifted to a lower frequency than in the pre-tilt O$_2$Hb spectrum. The post-tilt time series in both MAP and O$_2$Hb for the healthy subject show a single peak in the power spectrum which is at a similar frequency to the peak in the pre tilt case, albeit at higher power. It should be noted that peaks at frequencies higher than around 0.15 Hz are not significant in any of the power spectra.

Figure 3. Power spectral density of MAP and OHb for a typical control subject and an autonomic failure patient: (a) healthy subject MAP, (b) healthy subject O_2Hb, (c) autonomic failure patient MAP and (d) autonomic failure patient O_2Hb.
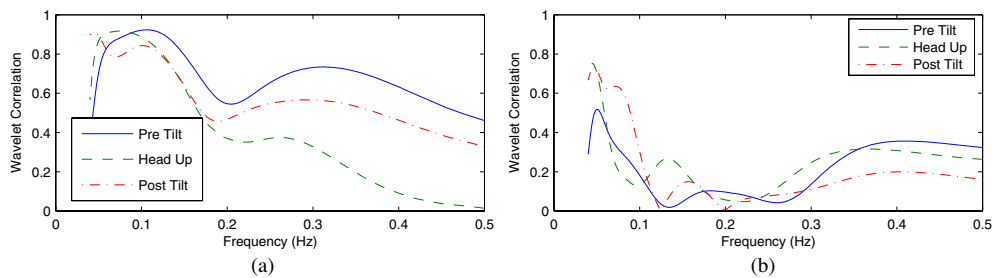
Figure 4. Value of wavelet cross-correlation between MAP and O_2Hb at zero time delay for a typical control subject and an autonomic failure patient. For comparison with figure 3, the wavelet scale has been converted to frequency using $f = \frac{10}{a}$: (a) healthy subject and (b) autonomic failure patient.

For the autonomic failure patient (figures 3(c) and (d)) peaks in the power spectra tend to be most pronounced at lower frequencies (<0.05 Hz) than in the healthy subject. For the MAP time series (figure 3(c)), both the pre-tilt and head-up power spectra show a secondary peak at slightly higher frequencies, however this is not reflected in either of the O_2Hb spectra.

Figure 4 shows the value of the wavelet cross-correlation between MAP and O_2Hb at a lag time of zero plotted versus frequency for direct comparison with the power spectral density plots in figure 3. For the control subject (figure 4(a)) we see two peaks, the first corresponding to a frequency of 0.1 Hz, the second to a frequency of ~0.3 Hz. These results for healthy elderly control subjects are in general agreement with the results of Latka *et al* (2005) for younger control subjects. Head-up tilt in the control subject causes the value of wavelet cross-correlation at the 0.3 Hz peak to diminish. For the autonomic failure patient (figure 4(b)), the strongest peak in wavelet cross-correlation appears at a frequency of around 0.05 Hz, for all postures. Head-up tilt causes the value of the wavelet cross-correlation at this
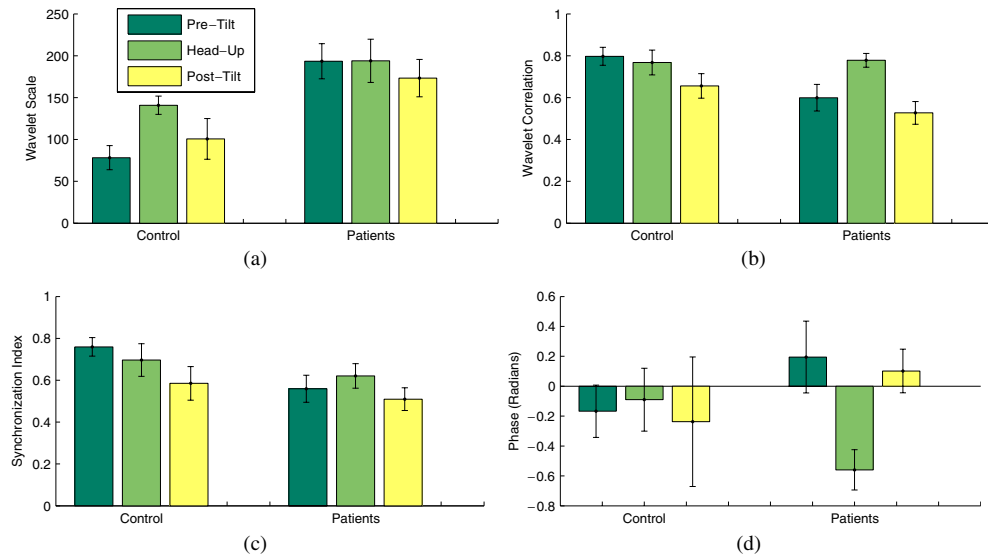
Figure 5. Group statistical analysis at maximum wavelet correlation of scale, value of correlation, synchronization index and circular mean phase difference. Error bars indicate standard deviation: (a) wavelet scale, (b) maximum wavelet correlation, (c) synchronization index and (d) circular mean phase.

frequency to increase. An important difference between the wavelet synchronization analysis and power spectral density analysis can be illustrated by considering the peak that is typically observed at the respiratory frequency of 0.3 Hz. Figure 3 shows no discernible peaks in the *power spectral density* of O_2Hb or MAP at 0.3 Hz, whereas figure 4 shows strong values of *wavelet cross-correlation* in this frequency range. Wavelet cross-correlation is a measure of the level of similarity between two signals in a given frequency band and does not depend upon the power of those signals provided that the time series are compared for a sufficiently long time interval.

Figure 5 shows the mean and standard deviation for indices obtained from the wavelet cross-correlation analysis for both subject groups at each posture. Figure 5(a) shows that for the control subjects a statistically significant increase in the mean value of scale at maximum wavelet cross-correlation occurs on assuming the upright posture ($p = 0.0038$). Upon returning to the supine position after the tilt, the group mean of the scales of maximum wavelet cross-correlation decreases again to a level similar to the pre-tilt value. In patients suffering from autonomic failure this change is not observed ($p = 0.9895$).

Figure 5(b) shows the value of the maximum wavelet cross-correlation. In all test subjects this was observed to be greater than 0.5. It can be seen that the value is typically lower in autonomic failure patients than in healthy subjects ($p = 0.0238$ patient pre-tilt versus control pre-tilt) although it increases on head-up tilt for patients ($p = 0.0236$), returning to a level similar to the pre-tilt value after the tilt. In healthy subjects this change is not observed.

Figure 5(c) shows the synchronization index (equation (3)) statistics for all subjects in the study. No significant differences between subject groups or with posture can be observed, although it should be noted that this index is again typically above 0.5 indicating synchronization at this scale.

Figure 5(d) shows the group statistics for the circular mean phase difference between MAP and O_2Hb (equation (2)). The variance in this index is quite large, illustrating its variability
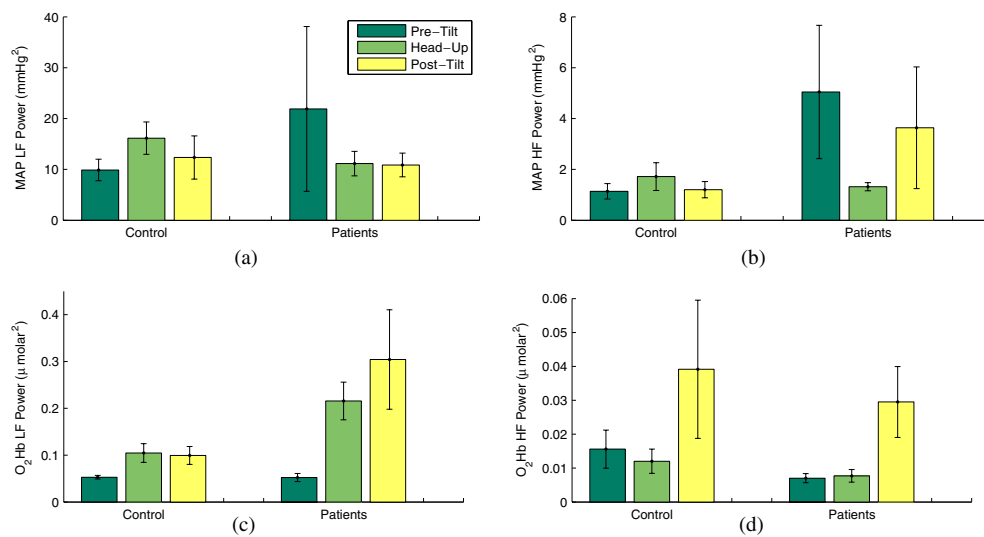
Figure 6. Group statistical analysis of low-frequency (<0.15 Hz) and high-frequency (>0.15 Hz) spectral power in MAP and O_2Hb. Error bars indicate standard deviation: (a) LF MAP total power, (b) HF MAP total power, (c) LF O_2Hb total power and (d) HF O_2Hb total power.

across subjects and with posture. Interestingly, for control subjects the group mean is negative for all postures, whereas for sympathetic failure patients the mean is negative only during head-up tilt ($p = 0.0145$ patient pre-tilt versus patient head-up; $p = 0.0043$ patient head-up versus patient post-tilt). A negative mean phase indicates that oscillations in O_2Hb occur *before* those in MAP. This finding, although controversial, is in agreement with the results of Cencetti *et al* (1999) and Zhang *et al* (2002).

Figure 6 shows the group statistics for the power spectral density analysis. The large error bars indicate the variability that is typically encountered in power spectra measured from patients and controls. The only statistically significant differences were the increase in LF O_2Hb power for autonomic failure patients ($p = 0.0011$) and controls ($p = 0.0234$) when assuming the head-up posture. This was previously reported in a different study (Tachtsidis *et al* 2004). It is possible that confidence in the results obtained from power spectral analysis could be increased with a longer duration test and a larger patient sample.

5. Discussion

Wavelet cross-correlation (WCC) between MAP and O_2Hb time series has been computed for elderly autonomic failure patients and age-matched controls in the supine position and during head-up tilt using a tilt table test. For healthy subjects in the supine position WCC typically exhibits two peaks, the first at a scale corresponding to a frequency of around 0.33 Hz, the second at a frequency of around 0.1 Hz. In healthy subjects passive head-up tilt using a tilt table causes the 0.33 Hz peak to disappear and the 0.1 Hz peak to shift to higher wavelet scales ($p = 0.0038$). For autonomic failure patients in the supine position the 0.33 Hz peak is not significant, and the LF peak typically occurs at a frequency lower than 0.1 Hz. In patients, head-up tilt does not cause a statistically significant shift in the low-frequency peak ($p = 0.9859$).

Power spectral analysis showed that increases in low-frequency power in O_2Hb can be observed in both patients ($p = 0.0011$) and controls ($p = 0.0234$) when they assume the upright posture in agreement with Tachtsidis *et al* (2004). No statistically significant changes in LF MAP power were observed, probably reflecting the large variability observed in our patient group for LF MAP power (see the error bars in figure 6(a)). It is not unreasonable to expect that this sort of variability is inherent to this patient group, for the short-duration tests that are practical to obtain in a clinical setting.

Cerebral autoregulation broadly describes the mechanism which couples systemic variables (heart-rate, MAP) to cerebral haemodynamic variables (e.g. O_2Hb). This coupling is due to the cooperative action of both sympathetically mediated and local myogenic mechanisms. It is thought that myogenic mechanisms act to buffer small changes in cerebral blood flow due to changes in systemic variables and that the sympathetic nervous system is most active during large pressure changes (Harper *et al* 1972). In autonomic failure patients it is possible that the sympathetic mechanisms of cerebral autoregulation are impaired and investigation of the relationship between systemic variables and cerebral haemodynamics could provide valuable diagnostic information in these patients. The inherent problem is that both systems exhibit considerable low-frequency variability and it is difficult to attribute the frequency content of the signals to any one mechanism even within a narrow frequency band. This may be illustrated by considering figures 3(a) and (c): in the low-frequency region MAP shows relatively broad spectral content below 0.1 Hz in both controls and autonomic failure patients. Figures 3(b) and (d) show that the O_2Hb frequency content is similarly variable in this range.

Many previous attempts to quantify the dynamics of cerebral autoregulation (see Panerai (1998)) have done so using a system identification technique which essentially involves division of the power spectra of MAP and TCD-measured VMCA resulting in a complex transfer function expressing the gain and phase of the system as a function of frequency. This makes the assumption that the entire frequency content of cerebral haemodynamic variables can be attributed to driving by systemic frequency content. The assumption of stationarity (that the relationship between the two time series remains relatively constant over time) is also required. Recent studies demonstrating changes in TCD-measured VMCA during functional studies (Panerai *et al* 2005) underline the limitations of these assumptions. It is also reasonable to expect that in autonomic failure patients in a clinical setting the assumption of stationarity could be confounded by the effect of experimental noise and the need to take a very short-duration test in order to minimize patient discomfort.

Wavelet cross-correlation decomposes the MAP and O_2Hb signals into wavelet modes which are highly localized in frequency and allows investigation of which modes are most linearly related. It makes no assumption about the stationarity of the relationship between the time series, and if other modes in cerebral haemodynamics exist which are not the result of driving by systemic variables these will show a low value of wavelet cross-correlation. Investigation of the scale at which wavelet cross-correlation has its maximum has shown that on head-up tilt in healthy subjects the frequency at which maximum wavelet cross-correlation occurs decreases. In autonomic failure patients this frequency is lower than in controls and does not show a statistically significant shift with posture. Consideration of the circular mean phase measured using wavelet analysis has shown that in controls, O_2Hb typically leads MAP, and shows no statistically significant differences with posture. In patients suffering from failure of the sympathetic nervous system in the supine position, O_2Hb phase lags MAP phase however when the patients assume the upright posture, O_2Hb shows a statistically significant phase lead with respect to MAP.

These results may be explained with reference to the physiology of the patient groups as follows: cardiovascular oscillations around a frequency of 0.1 Hz are thought to be a marker of sympathetic control of circulation. The observed phase lead of the wavelet components of O_2Hb with respect to MAP at maximum cross-correlation in control subjects for all postures in the supine posture suggests that these components reflect neural control of the cerebral circulation. In patients in the supine position O_2Hb lagging MAP indicates passive stimulation of the cerebral circulation by low-frequency content in blood pressure (Cencetti *et al* 1999). When patients assume the upright posture, this does not cause the frequency of maximum correlation to change much, however phase changes at this frequency from O_2Hb lagging MAP to O_2Hb leading MAP, as is the case for control subjects in all postures. In control subjects the statistically significant shift in the scale of maximum correlation indicates that the sympathetic mechanism is indeed challenged by the change in posture. However, the fact that the phase lead of O_2Hb with respect to MAP is preserved throughout the test suggests that neural control is maintained even upon head-up tilt and explains why syncope is rarely observed in these patients. In sympathetic failure patients the O_2Hb phase lag suggests impaired sympathetic regulation. On head-up tilt some mechanism is activated to cause phase lead yet this is not sufficient in many cases to prevent syncope.

The results of this study for healthy subjects are in agreement with the results of Latka *et al* (2005) who investigated synchronization between MAP and TCD-measured middle cerebral artery blood flow velocity using complex Morlet wavelets for ten healthy young subjects and observed significantly reduced circular phase variance around 0.33 Hz and 0.1 Hz. Our study represents the first time that wavelet cross-correlation has been used to investigate the posture dependence of synchronization between MAP and NIRS-measured O_2Hb in elderly autonomic failure patients in comparison with age-matched controls.

6. Conclusion

LF oscillations in cerebral O_2Hb measured using single-channel NIRS have been related to LF oscillations in systemic MAP measured non-invasively using finger photoplethysmography by investigating wavelet cross-correlation between the two time series. This analysis has been performed for elderly patients suffering from autonomic failure and healthy age-matched controls. It has been shown that the frequency of maximum wavelet cross-correlation is significantly different for patients with respect to controls. We argue that synchronization analysis provides information which is fundamentally different from the comparison of power spectra.

Estimation of the phase relationship between the two sources of oscillation using the complex continuous wavelet transform has demonstrated the variability of this measure in the patient group considered. This suggests that the assumption of stationarity and transfer function analysis may produce confusing results in elderly subjects and those suffering from autonomic failure.

Investigation of the spectral properties of LF oscillations in cerebral haemodynamics and their relationship to other variables (both global cardiovascular variability and local cerebral effectors) is important in understanding the sources of physiological 'noise' in functional imaging experiments and in the diagnosis of patients with autonomic failure. It is suggested that further work should investigate the applicability of this technique to the analysis of low-frequency synchronization of cerebral haemodynamics with other potential sources of low-frequency variability in cardiovascular parameters, for example low-frequency fluctuations in the partial pressure of end-tidal carbon dioxide (PET_{CO_2}).

Acknowledgments

References

Cencetti S, Lagi A, Cipriani M, Fattorini L, Bandinelli G and Bernardi L 1999 Autonomic control of the cerebral circulation during normal and impaired peripheral circulatory control *Heart* **82** 365–72

Chandler M P and Mathias C J 2002 Haemodynamic responses during head-up tilt and tilt reversal in two groups with chronic autonomic failure: pure autonomic failure and multiple system atrophy *J. Neurol.* **249** 542–8

Cohen M A and Taylor J A 2002 Short-term cardiovascular oscillations in man: measuring and modelling the physiologies *J. Physiol.* **542** 669–83

Delpy D T and Cope M 1997 Quantification in tissue near-infrared spectroscopy *Phil. Trans. R. Soc.* B **352** 649–59

Elghozi J L, Laude D and Janvier F 1991 Clonidine reduces blood pressure and heart rate oscillations in hypertensive patients *J. Cardiovasc. Pharmacol.* **17** 935–40

Elwell C E, Springett R, Hillman E and Delpy D T 1999 Oscillations in cerebral haemodynamics. Implications for functional activation studies *Adv. Exp. Med. Biol.* **471** 57–65

Fisher N I 1995 *Statistical Analysis of Circular Data* (Cambridge: Cambridge University Press)

Giller C A, Hatab M R and Giller A M 1999 Oscillations in cerebral blood flow detected with a transcranial Doppler index *J. Cereb. Blood Flow Metab.* **19** 452–9

Giller C A and Mueller M 2003 Linearity and non-linearity in cerebral hemodynamics *Med. Eng. Phys.* **25** 633–46

Goulden C H 1959 *Methods of Statistical Analysis* (*Wiley Publications in Statistics*) (New York: Wiley)

Grinsted A, Moore J C and Jevrejeva S 2004 Application of the cross wavelet transform and wavelet coherence to geophysical time series *Nonlinear Process. Geophys.* **11** 561–6

Haddock R E and Hill C E 2005 Rhythmicity in arterial smooth muscle *J. Physiol.* **566** 645–56

Harper A M, Deshmukh V D, Rowan J O and Jennett W B 1972 The influence of sympathetic nervous activity on cerebral blood flow *Arch. Neurol.* **27** 1–6

Hu X, Nenov V, Glenn T C, Steiner L A, Czosecondnameyka M, Bergsecondnameeider M and Martin N 2006 Nonlinear analysis of cerebral hemodynamic and intracranial pressure signals for characterization of autoregulation *IEEE Trans. Biomed. Eng.* **53** 195–209

Hudetz A G, Roman R J and Harder D R 1992 Spontaneous flow oscillations in the cerebral cortex during acute changes in mean arterial pressure *J. Cereb. Blood Flow Metab.* **12** 491–9

Jaradeh S S and Prieto T E 2003 Evaluation of the autonomic nervous system *Phys. Med. Rehabil. Clin. N. Am.* **14** 287–305

Kamiya A *et al* 2005 Low-frequency oscillation of sympathetic nerve activity decreases during development of tilt-induced syncope preceding sympathetic withdrawal and bradycardia *Am. J. Physiol. Heart Circ. Physiol.* **289** H1758–69

Kawaguchi T, Uyama O, Konishi M, Nishiyama T and Iida T 2001 Orthostatic hypotension in elderly persons during passive standing: a comparison with young persons *J. Gerontol. A: Biol. Sci. Med. Sci.* **56** M273–80

Latka M, Turalska M, Glaubic-Latka M, Kolodziej W, Latka D and West B J J 2005 Phase dynamics in cerebral autoregulation *Am. J. Physiol. Heart Circ. Physiol.* **289** H2272–9

Le Van Quyen M, Foucher J, Lachaux J, Rodriguez E, Lutz A, Martinerie J and Varela F J 2001 Comparison of Hilbert transform and wavelet methods for the analysis of neuronal synchrony *J. Neurosci. Methods* **111** 83–98

Malliani A, Pagani M, Lombardi F and Cerutti S 1991 Cardiovascular neural regulation explored in the frequency domain *Circulation* **84** 482–92

Maraun D and Kurths J 2004 Cross wavelet analysis: significance testing and pitfalls *Nonlinear Process. Geophys.* **11** 505–14

Mayer S 1876 Studien zur Physiologie des Herzens und der Blutgefässe: 6. Abhandlung: ber spontane Blutdruckschwankungen *Sitzungsberichte Akademie der Wissenschaften in Wien. Mathematisch-naturwissenschaftliche Classe, Anatomie* **74** 281–307

Mayhew J E, Askew S, Zheng Y, Porrill J, Westby G W, Redgrave P, Rector D M and Harper R M 1996 Cerebral vasomotion: a 0.1-Hz oscillation in reflected light imaging of neural activity *Neuroimage* **4** 183–93

Misiti M, Misiti Y, Oppenheim G and Poggi J M 2004 *Matlab Wavelet Toolbox User's Guide* version 3 (Natick, MA: The Mathworks, Inc.)

Mitsis G and Marmarelis V 2002 Modeling of nonlinear physiological systems with fast and slow dynamics: I. Methodology *Ann. Biomed. Eng.* **30** 272–81

Mitsis G D, Poulin M J, Robbins P A and Marmarelis V Z 2004 Nonlinear modeling of the dynamic effects of arterial pressure and CO$_2$ variations on cerebral blood flow in healthy humans *IEEE Trans. Biomed. Eng.* **51** 1932–43

Mitsis G, Zhang R, Levine B and Marmarelis V 2002 Modeling of nonlinear physiological systems with fast and slow dynamics: II. Application to cerebral autoregulation *Ann. Biomed. Eng.* **30** 555–65

Mizuno-Matsumoto Y, Ukai S, Ishii R, Date S, Kaishima T, Shinosaki K, Shimojo S, Takeda M, Tamura S and Inouye T 2005 Wavelet-crosscorrelation analysis: non-stationary analysis of neurophysiological signals *Brain Topogr.* **17** 237–52

Nilsson H and Aalkjaer C 2003 Vasomotion: mechanisms and physiological importance *Mol. Interv.* **3** 79–89

Obrig H, Neufang M, Wenzel R, Kohl M, Steinbrink J, Einhupl K and Villringer A 2000 Spontaneous low frequency oscillations of cerebral hemodynamics and metabolism in human adults *Neuroimage* **12** 623–39

Pagani M, Lombardi F, Guzzetti S, Rimoldi O, Furlan R, Pizzinelli P, Sandrone G, Malfatto G, Dell'Orto S and Piccaluga E 1986 Power spectral analysis of heart rate and arterial pressure variabilities as a marker of sympatho–vagal interaction in man and conscious dog *Circ. Res.* **59** 178–93

Panerai R B 1998 Assessment of cerebral pressure autoregulation in humans—a review of measurement methods *Physiol. Meas.* **19** 305–38

Panerai R B, Dawson S L, Eames P J and Potter J F 2001 Cerebral blood flow velocity response to induced and spontaneous sudden changes in arterial blood pressure *Am. J. Physiol. Heart Circ. Physiol.* **280** H2162–74

Panerai R B, Moody M, Eames P J and Potter J F 2005 Cerebral blood flow velocity during mental activation: interpretation with different models of the passive pressure–velocity relationship *J. Appl. Physiol.* **99** 2352–62

Panerai R B, White R P, Markus H S and Evans D H 1998 Grading of cerebral dynamic autoregulation from spontaneous fluctuations in arterial blood pressure *Stroke* **29** 2341–6

Schatz I J *et al* 1996 Consensus statement on the definition of orthostatic hypotension, pure autonomic failure, and multiple system atrophy *J. Neurol. Sci.* **144** 218–9

Simpson D M, Panerai R B, Evans D H and Naylor A R 2001 A parametric approach to measuring cerebral blood flow autoregulation from spontaneous variations in blood pressure *Ann. Biomed. Eng.* **29** 18–25

Stauss H M, Anderson E A, Haynes W G and Kregel K C 1998 Frequency response characteristics of sympathetically mediated vasomotor waves in humans *Am. J. Physiol.* **274** H1277–83

Tachtsidis I, Elwell C E, Lee C W, Leung T S, Smith M and Delpy D T 2003 Spectral characteristics of spontaneous oscillations in cerebral haemodynamics are posture dependent *Adv. Exp. Med. Biol.* **540** 31–6

Tachtsidis I, Elwell C E, Leung T S, Bleasdale-Barr K, Hunt K, Toms N, Smith M, Mathias C J and Delpy D T 2005 Rate of change in cerebral oxygenation and blood pressure in response to passive changes in posture: a comparison between pure autonomic failure patients and controls *Adv. Exp. Med. Biol.* **566** 187–93

Tachtsidis I, Elwell C E, Leung T S, Lee C W, Smith M and Delpy D T 2004 Investigation of cerebral haemodynamics by near-infrared spectroscopy in young healthy volunteers reveals posture-dependent spontaneous oscillations *Physiol. Meas.* **25** 437–45

Townsend N W and Germuska R B 2005 Locating features in a photoplethysmoraph signal US Patent Application 10/490,545

Welch P D 1967 The use of fast Fourier transform for the estimation of power spectra: a method based on time averaging over short, modified periodograms *IEEE Trans. Audio Electroacoust.* **15** 70–3

Zhang R, Zuckerman J H, Iwasaki K, Wilson T E, Crandall C G and Levine B D 2002 Autonomic neural control of dynamic cerebral autoregulation in humans *Circulation* **106** 1814–20